

A 3–5 GHz TH-UWB transmitter in 0.18- μm RF CMOS technology*

Duan Jihai(段吉海)^{1,2,†}, Wang Zhigong(王志功)¹, and Li Zhiqun(李智群)¹

(1 School of Integrated Circuits, Southeast University, Nanjing 210096, China)

(2 School of Information & Communication, Guilin University of Electronic Technology, Guilin 541004, China)

Abstract: An RF transmitter is proposed for 3–5 GHz time-hopping ultra wideband (TH-UWB) wireless applications. The transmitter consists of a 4-GHz oscillator, a switch with a controllable attenuator and an output matching circuit. Through controlling the low frequency signals with time-hopping pulse position modulation (TH-PPM), the circuit supplies TH-UWB signals and can directly drive an antenna by a transmission line. The transmitter was implemented in a 0.18- μm CMOS technology; the output amplitude is about 65 mV at a 50 Ω load from a 1.8-V supply, the return loss (S_{11}) at the output port is less than -10 dB, and the chip size is $0.7 \times 0.8 \text{ mm}^2$, with a power consumption of 12.3 mW.

Key words: complementary metal oxide semiconductor; transmitter; time-hopping ultra wideband

DOI: 10.1088/1674-4926/30/7/075006

EEACC: 1230

1. Introduction

Ultra-wideband (UWB) systems are particularly promising for short-range wireless communications as they potentially combine a reduced complexity with a low power consumption, a low probability of intercept (LPI), and the immunity to multi-path fading^[1–3]. Two possible approaches have emerged to exploit the allocated spectrum. One is the multi-band approach, with fourteen 500-MHz sub-bands of OFDM modulation, and the other is the impulse radio^[4].

According to the physical layer standard of IEEE 802.15.3a^[5] regulated by the US Federal Communications Commission (FCC), the allocated frequency band for UWB applications is 3.1–10.6 GHz. The lower frequency band and the higher frequency band refer to 3–5 GHz and 6–10.6 GHz, respectively. The supporting modulation schemes include direct-sequence UWB (DS-UWB) and multi-band orthogonal frequency division multiplexing (MB-OFDM)^[6].

Recently, several pulse generating approaches were proposed for UWB communications. In Ref. [7], a simple digital circuit is used to generate narrow pulses. In Ref. [8], a triangular pulse generator and a ring oscillator are activated simultaneously. A gating circuit activates the ring oscillator when a pulse must be transmitted, avoiding useless power consumption between the pulses. Reference [9] also uses a programmable time delay circuit and an oscillator to generate UWB pulse signals.

In this paper, a novel TH-UWB transmitter is proposed. The transmitter works at a center frequency of 4 GHz with multi-pulse UWB signals, which meets the requirement of frequency bandwidth and maximal radiated power of FCC. A controllable CMOS switch and an oscillator are used to generate TH-UWB pulses. This CMOS switch does not dissipate any static power. Moreover, the output voltage amplitude of

the transmitter is controlled easily by the TH-PPM pulses.

2. Design requirements

The maximal radiated power of the required transmitter is lower than -41.3 dBm/MHz with respect to the standard of IEEE 802.15.3a. The attributes required for the design were as follows:

- (1) The output amplitude is about 65 mV at a 50 Ω load from a 1.8-V supply (in consideration of the insertion loss between the transmitter and the antenna, and the attenuation of the antenna).
- (2) The output impedance is matched to 50 Ω , and the return loss (S_{11}) is less than -10 dB over 3–5 GHz.
- (3) The modulation signal is TH-PPM with a pulse width of less than 4 ns.
- (4) The modulated signal is a TH-UWB signal with a multi-pulse, which is realized by an OOK (on-off keying) modulator with a 4-GHz carrier frequency.
- (5) Low power dissipation.
- (6) Minimum die area.

3. Circuit description

3.1. TH-PPM and TH-UWB pulses

In a typical TH-UWB system, the transmitted signal by user k can be expressed as^[10–13]

$$s_{\text{TH}}^k(t) = \sum_{i=-\infty}^{+\infty} \sum_{j=0}^{N_f-1} b_i p(t - c_{\text{th},j}^k T_c - iT_s), \quad (1)$$

where N_f is the number of frames in each symbol, T_s is the symbol time, T_s represents the frame duration, and T_c is the chip duration. If we consider that there are N_c chips in each

* Project supported by the National High Technology Research and Development Program of China (No. 2007AA03Z454) and the Science Foundation of Guangxi Province, China (No. 0575096).

† Corresponding author. Email: djh@guet.edu.cn

Received 2 February 2009, revised manuscript received 25 March 2009

© 2009 Chinese Institute of Electronics

frame, then $N_f = N_c T_c$. c_{th} represents the hopping code, which can take any integer value between 0 and N_{c-1} . $p(t)$ is the pulse shape function.

Because the frequency band allocated by FCC for UWB applications is 3.1–10.6 GHz, traditional Gaussian pulses, Gaussian monocycle pulses, and Scholtz pulses cannot match the criteria of the FCC frequency spectrum. It is necessary to move the traditional UWB pulse's frequency spectrum to the range of 3.1–10.6 GHz.

In this paper, we utilize the technology of Armstrong beat frequency, i.e., the OOK modulation. Two different pulse shapes have been used as TH-PPM signals: rectangle and Gaussian pulses as shown in Eqs. (2) and (3), respectively^[6].

$$p(t) = \begin{cases} 1, & -\frac{T}{2} < t < \frac{T}{2}, \\ 0, & \text{otherwise,} \end{cases} \quad (2)$$

$$p(t) = \begin{cases} Ke^{-(t/\tau)^2}, & -\frac{T}{2} < t < \frac{T}{2}, \\ 0, & \text{otherwise.} \end{cases} \quad (3)$$

We also use an oscillator to generate a cosine signal as a carrier signal. Through an OOK modulation, we can acquire the TH-UWB signal, which meets the FCC standard frequency bandwidth. The modulated signal waveform is expressed as

$$S_{TH-UWB}(t) = \sum_{i=-\infty}^{+\infty} \sum_{j=0}^{N_f-1} b_i \cos(2\pi f_0 t) \times p(t - c_{th,j} T_c - jT_s), \quad (4)$$

where $\cos(2\pi f_0 t)$ represents the carrier signal for the OOK modulation.

3.2. System design

The transmitter, as shown in Fig. 1, has a 4-GHz oscillator, a switch with a controllable attenuator, and an output matching circuit. Here the ‘‘Oscillator’’ generates a sinusoidal signal at a frequency of 4 GHz. The signal is used as a carrier in the OOK modulation. The ‘‘CMOS controllable attenuator switch’’ serves as an OOK digital modulator and it can move the signal frequency spectrum from the PPM signal to the center frequency of 4 GHz so as to meet the standard of IEEE 802.15.3a, the ‘‘Matching network’’ matches the output impedance of the UWB signal generator to 50 Ω.

3.3. Circuit design

In terms of the idea of the system scheme in Fig. 1, the schematic of the designed TH-UWB transmitter is shown in Fig. 2. An active LC negative resistance circuit (M_3, M_4, C_1 , and L_1) is used as the ‘‘Oscillator’’ in Fig. 1 with an oscillating frequency around 4 GHz. M_6 is used for the output buffering. The proposed circuit is biased by a current source (M_1, M_2, M_5 , and R_1). A MOSFET transmission gate (M_7, M_8 , and M_{11}) acts as the ‘‘CMOS controllable attenuator switch’’ in Fig. 1. M_9 and M_{10} build up an inverter, which offers the controlling signal to the CMOS switch. The attenuated value is controlled by the level of the PPM input signal. As the controlling signal at the gate is a voltage signal, so it is in possession

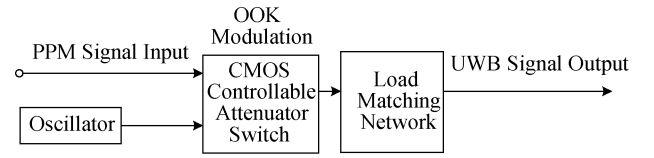


Fig. 1. Principle diagram of the TH-UWB transmitter.

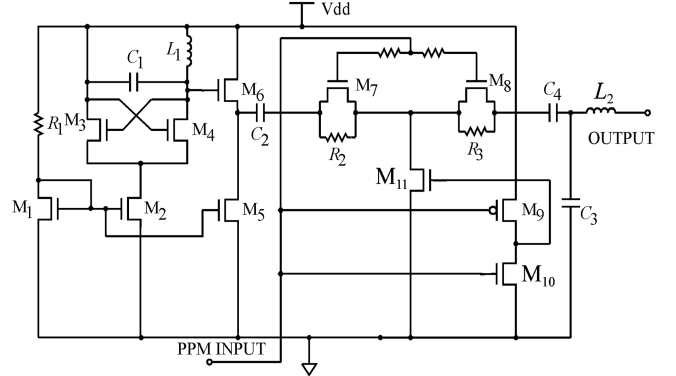


Fig. 2. Circuit of the TH-UWB transmitter.

of a good switch characteristic. In order to design the insertion loss and the maximum attenuation, some parasitic parameters should be considered as follows:

(1) This attenuator is a T-type network. In a T-attenuator like this, a minimum attenuation occurs when the series device is completely on and the shunt devices are off. In that case, the loss at low frequencies comes only from the nonzero on-resistance of the series device. As this resistor gets smaller, the signal loss due to the insertion of the attenuator gets smaller. At higher frequencies, there is additional loss caused by the parasitic capacitors to ground, and minimizing these capacitors reduces the loss.

(2) The parasitic capacitors in the T-attenuator are functions of the biasing of the transistors and, therefore, are different in values from the minimum attenuation case^[14].

The ‘‘Load matching network’’ in Fig. 1 is designed in an L-type matching network (C_3 and L_2). C_2 and C_4 are used for coupling.

Defining the transconductance of M_3 and M_4 as g_{m3} and g_{m4} , respectively, and with $g_{m3} = g_{m4} = g_m$, the whole negative impedance should be $-2/g_m$ ^[15]. A steadily going oscillator requires that the loss of the LC resonance circuit should counteract the negative impedance, so the oscillating condition is

$$R_{eq} \geq 2/g_m, \quad (5)$$

where R_{eq} is the equivalent parallel resistance of the LC resonance circuit.

3.4. Impedance matching

In order to match the output impedance to the load, the Smith chart is used for impedance analysis on a certain frequency band, and an L-type network composed of C_3 and L_2 is adopted. Assuming that the serial admittance is G_S/jB_S , the parallel admittance is $G_P + jB_P$, the real parts are the same, and

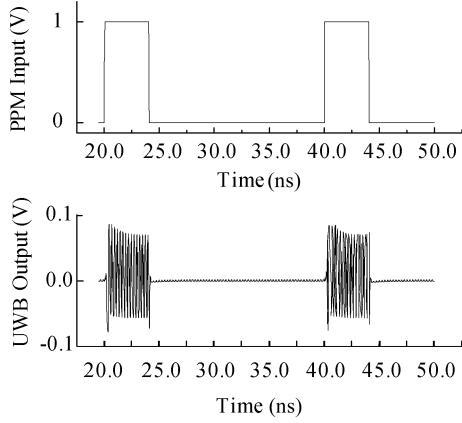


Fig. 3. Simulation waveforms.

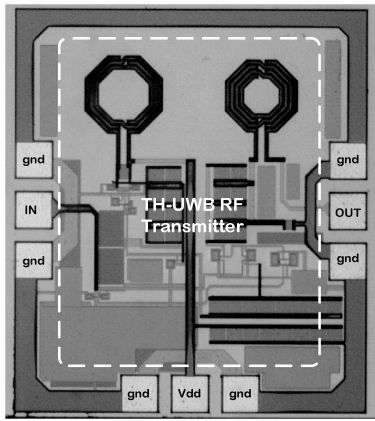


Fig. 4. Die photograph.

the imaginary parts are reverse, there are formulas as follows^[16]:

$$1 + Q^2 = \frac{G_S}{G_P}, \tag{6}$$

$$Q = \frac{G_S}{B_S}, \tag{7}$$

$$Q = \frac{B_P}{G_P}. \tag{8}$$

Utilizing a Smith chart to simulate the unmatched port, we can get $G_P = 1/R_P$ at 4 GHz. Then, Q , B_S , B_P can be calculated. Because B_S and B_P are related to L_2 and C_3 in Fig. 2, respectively, L_2 and C_3 can be calculated.

4. Simulation and measurement

Under the environment of the SMIC 0.18- μm CMOS process, the impedance matching was made by using Cadence tools and S_{11} was obtained when the output impedance is matched, as shown in Fig. 7. The sweeping range of the frequency is from 3 GHz to 5 GHz. The simulation result in Fig. 7 shows that the value of S_{11} is less than -10 dB in the whole bandwidth. After the determination of the circuit parameter and impedance matching, a schematic simulation for the circuit in Fig. 2 was carried out in SMIC's 0.18- μm CMOS process, and the results are shown in Fig. 3 (with a pulse width of 4 ns and a period of 20 ns for the PPM signals controlling the UWB signal generator). It shows that the amplitude is about 65 mV, and the carrier frequency is 4 GHz.

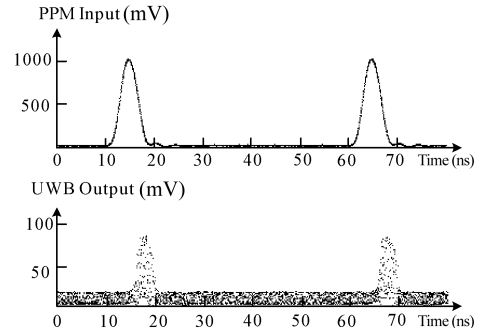


Fig. 5 Measured waveforms.

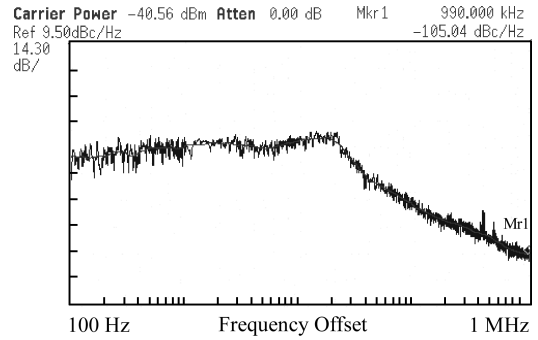


Fig. 6. Measured phase noise.

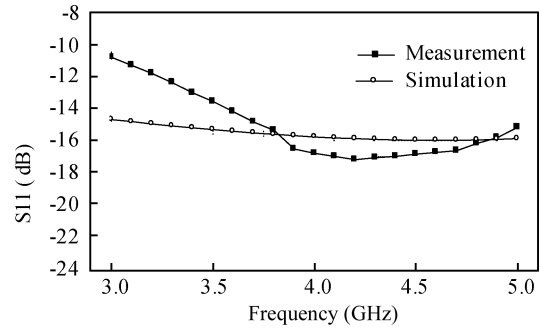


Fig. 7. Simulated and measured S_{11} .

The transmitter is implemented in SMIC's 0.18- μm RF CMOS. The die area is $0.7 \times 0.8 \text{ mm}^2$ (Fig. 4), with a power consumption of 12.3 mW. Figure 5 shows the measured TH-PPM input signal and TH-UWB output signal. A Gaussian pulse-shape is used as a TH-PPM pulse and the TH-UWB output signal amplitude is about 65 mV. Both signals are measured by an Agilent infiniium DCA 86100A wide-bandwidth oscilloscope. Because the oscilloscope needs a carrier synchronizing signal, but there is not such a signal in this chip, only the envelope of the "UWB output" can be seen. The frequency from the oscillator measured by an Agilent E4440 frequency spectrum analyzer is 3.8769 GHz and the measured phase noise is shown in Fig. 6. The phase noise of the oscillator, which is measured by an Agilent E4440 frequency spectrum analyzer, is -105 dBc/Hz at a 1-MHz offset from the carrier. Compared with the simulation result, there is a difference of 123.1 MHz. This is because the proposed oscillator is not a VCO, and the process deviation is not taken into account. When we use an envelop detector to demodulate this signal, such a frequency deviation is insignificant.

Figure 7 shows the simulated and measured S_{11} at the output port. The simulated and measured results show that

Table 1. Performance summary and comparison with published works.

Specification	This work	Ref. [7]	Ref. [8]	Ref. [9]
Technology	0.18- μm CMOS	0.18- μm CMOS	0.18- μm CMOS	0.18- μm CMOS
Status	Measured	Measured	Measured	Simulation
Output (mV)	65	200	200	170
Supply voltage (V)	1.8	1.8	Unknown	1.8
Carrier frequency (GHz)	3.8769	No carrier	4.488	No carrier
Output matching (S_{11})	< -10 dB	Unknown	Unknown	Unknown
Power consumption (mW)	12.3	0.522	2	12.5

both values are less than -10 dB. From the results in Fig. 7, the simulated S_{11} is flattened over the given frequency range, i.e., with -14 to -16 dB. Compared with the simulated curve, the measured S_{11} has more difference, i.e., with -10 to -17 dB. This can also be ascribed to the affect of the parasitic parameters of the chip.

5. Conclusion

Through the circuit design, impedance matching, the pre-simulation and the measurement, the results meet the design requirement. The performance results for the proposed transmitter and a comparison with previously published design are summarized in Table 1.

Compared with the references in Table 1, this work has some differences: first, this work offers the output matching in order to link an antenna by a 50Ω transmission line; second, this work utilizes a T-type CMOS attenuator network to realize the OOK modulation so as to reduce the consumption of power; meanwhile, the output UWB signal spectrum is fully limited to the regular range of FCC.

References

- [1] Win M Z. Spectral density of random UWB signals. *IEEE Comm Lett*, 2002, 6(12): 526
- [2] Win M Z, Scholtz R A. Ultra-wide bandwidth signal propagation for indoor wireless communications. *IEEE International Conference on Communications MONTREAL*, Canada, 1997: 56
- [3] Laney D C, Maggioni G M. Multiple access for UWB impulse radio with pseudochaotic time hopping. *IEEE J Sel Areas Comm*, 2002, 20(9): 1692
- [4] Tang S K, Pun K P, Choy C S, et al. A fully differential low noise amplifier with real-time channel hopping for ultra-wideband wireless applications. *ISCAS*, 2006: 4507
- [5] Batra A, Balakrishnan J, Dabak A, et al. Multi-band OFDM physical layer proposal for IEEE 802.15 task group 3a. *IEEE P802.15-03/268r3*, March 2004
- [6] Siwiak K, Mckeown D. Ultra-wideband radio technology. Zhang Zhongzhao, Sha Xuejun, Translation. Beijing: Publishing House of Electronic Industry, 2004 (in Chinese)
- [7] Yuan T, Zheng Y, Ang C W, et al. A fully integrated CMOS transmitter for ultra-wideband applications. *Proc IEEE Radio Frequency Integrated Circuits (RF IC) Symposium*, 2007: 39
- [8] Rychaert J, Desset C, Fort A, et al. Ultra-wide-band transmitter for low-power wireless body area networks: design and evaluation. *IEEE Trans Circuits Syst I*, 2005, 52(12): 2515
- [9] Saha P K, Sasaki N, Kikkawa T. A CMOS UWB transmitter for intra/inter-chip wireless communication. *IEEE International Symposium on Spread Spectrum Techniques and Applications*, 2004: 962
- [10] Scholtz R A. Multiple access with time hopping impulse modulation. *Proc Military Communications Conference*, Boston, MA, 1993, 2: 447
- [11] Win M Z, Scholtz R A. Ultra-wide band time-hopping spread-spectrum impulse radio for wireless multiple access communications. *IEEE Trans Comm*, 2000, 48(4): 679
- [12] Win M Z, Scholtz R A. Comparison of analog and digital impulse radio for wireless multiple access communications. *IEEE International Conference on Communications*, Montreal, Canada, 1997: 91
- [13] Sarfaraz K, Ghavami M. Unified method for bit error rate calculation of time hopping and direct-sequence ultrawide band systems in the presence of multiple user interference and narrow-band interference. *IET Commun*, 2008, 2(9): 1141
- [14] Dogan H, Meyer R G, Nikejad A M. Analysis and design of RF CMOS attenuators. *IEEE J Solid-State Circuits*, 2008, 43(10): 2269.
- [15] Li Zhiquan, Wang Zhigong, Zhang Liguang. Low phase noise LC VCO design in CMOS technology. *Journal of Southeast University (English Edition)*, 2004, 20(1): 6
- [16] Misra D K. Radio-frequency and microwave communication circuits analysis design. 2nd ed. Zhang Zhaoyi, Xu Chenghe, Zhu Xili, Translation. Beijing: Publishing House of Electronic Industry, 2005 (in Chinese)